energies

MDPI

Article

Effect of Phase Change Materials on the Thermal Performance of Residential Building Located in Different Cities of a Tropical Rainforest Climate Zone

Almas Sheriyev, Shazim Ali Memon *, Indira Adilkhanova and Jong Kim

Department of Civil and Environmental Engineering, School of Engineering and Digital Sciences, Nazarbayev University, Nur-Sultan 010000, Kazakhstan; almas.sheriyev@alumni.nu.edu.kz (A.S.); indira.adilkhanova@alumni.nu.edu.kz (I.A.); jong.kim@nu.edu.kz (J.K.)
* Correspondence: shazim.memon@nu.edu.kz

Abstract: This study aims to investigate the thermal performance of *PCM* and *PCM* combined with nighttime natural (NV) and mechanical ventilation (MV) applied to a residential building located in eight cities of tropical rainforest climate zone (Af). The analysis was accomplished using numerical simulations and developing a unique methodology for selecting the *PCM* melting temperature based on the thermal comfort limits. The thermal performance of the *PCM* integrated building was quantitatively evaluated using the concept of peak temperature drop. Additionally, a novel indicator of Total Temperature Drop (*TTD*) was introduced to determine the overall impact of the *PCM* and *PCM* combined with NV/MV on the thermal comfort conditions inside the building. The results showed that *PCM* 28 was the most efficient in improving the thermal performance of the building located in the Af climate zone, achieving a *TTD* of up to 356 °C per year. The usage of *PCM* 28 combined with nighttime natural ventilation improved the *TTD* values by up to 15%, whereas the integration of *PCM* 28 combined with mechanical ventilation resulted in a *TTD* values increase of up to 45%. Conclusively, mechanical ventilation showed its superiority over natural ventilation in the tropical rainforest climate, and *PCM* 28 applied together with mechanical ventilation could be used as the optimum combination for the whole climate zone.

Keywords: Af climate zone; phase change materials; daily peak temperature drop; total temperature drop; natural ventilation; mechanical ventilation

Citation: Sheriyev, A.; Memon, S.A.; Adilkhanova, I.; Kim, J. Effect of Phase Change Materials on the Thermal Performance of Residential Building Located in Different Cities of a Tropical Rainforest Climate Zone. *Energies* **2021**, *14*, 2699. https://doi.org/10.3390/en14092699

Academic Editor: Fitsum Tariku

Received: 22 March 2021
Accepted: 26 April 2021
Published: 8 May 2021

1. Introduction

Due to fast-growing economic development and high living standards, a considerable increase in energy consumption can be observed worldwide. According to energy consumption reports, around 80% of the global energy consumed comes from fossil fuel combustion [1], which is the primary source of carbon dioxide emissions, significantly contributing to environmental pollution and climate change. The building sector is one of the main energy consumers and contributors to carbon dioxide emissions worldwide. It is responsible for over one-third of the final global energy consumption and 40% of global CO_2 emissions [2]. There are predictions that the amount of energy consumed by the building sector will keep on increasing due to more frequent use of energy-consuming devices, better access to energy in developing countries, and the growing construction of buildings worldwide [2]. Therefore, to reduce energy consumption and CO_2 emissions, it is crucial to develop renewable energy resources and adopt energy-efficient building designs. In recent years, *PCM* has attracted many researchers' attention as a potential tool for passive heating and cooling applications. PCMs represent a type of thermal energy storage materials that possess a large amount of energy during their phase change process [3,4]. With their extensive latent heat storage capacity, they increase the building's thermal mass, making the indoor temperature more stable [5,6].

There are numerous studies about the thermal performance of PCM-integrated buildings in different climates of the world [7–10]. For example, Zhou et al. [7] numerically analyzed the effect of the shape-stabilized *PCM* (SSPCM) plates incorporated into the walls and ceiling on the inside temperature of a building located in Beijing, China. The authors revealed that varying thermophysical properties of SS*PCM* and incorporating daytime natural ventilation and nighttime mechanical ventilation reduced the indoor maximum temperature by up to 2 °C. Alam et al. [8] conducted a comparative analysis of passive and free cooling application methods of *PCM* integration into the building. The numerical study undertaken for Melbourne's climate demonstrated that the passive method of integration of Bio*PCM* reduced the indoor maximum temperature by up to 0.44 °C, and a free cooling application of *PCM* resulted in a peak temperature reduction of up to 2.63 °C. The effectiveness of applying *PCM* together with natural ventilation was analyzed by Zhang et al. [9]. The authors evaluated the effect of *PCM* combined with natural ventilation on the building's energy efficiency and thermal performance in five cities of China. The study results suggested that, in comparison with daytime ventilation, the nighttime ventilation was more effective in improving the thermal performance of the building integrated with *PCM*. The authors concluded that a higher air change rate of ventilation resulted in better thermal performance of *PCM*. Evola et al. [10] studied the impact of *PCM* on the thermal performance of the lightweight building during summertime for the climate of Chambery, France. The results showed that the application of the *PCM* notably improved thermal conditions inside the building, achieving a peak temperature reduction of up to 0.9 °C. Jamil et al. [11] examined the PCM's thermal performance applied to a building located in Melbourne, Australia. The authors conducted both experimental and numerical analyses. The data obtained showed that the incorporation of the *PCM* resulted in an inside temperature decrease of up to 1.1 °C. Additionally, based on the results obtained, it was concluded that the incorporation of natural nighttime ventilation considerably enhanced the performance of the *PCM*. Li et al. [12] numerically investigated the impact of a PCM-integrated roof on a building's thermal performance located in Northeast China. Based on the data obtained, the authors revealed that a *PCM* application to the roof significantly affected the thermal comfort conditions, shifting the peak temperature by up to 3 h. In the study by Ahangari and Maerefat [13], about PCM-integrated buildings located in different climates of Iran, the authors proposed a double-*PCM* layer system as an innovative solution for improving both the thermal and energy performances. The results demonstrated that the double-layer *PCM* system notably improved the thermal comfort conditions, increasing the duration of the thermal comfort by up to 20% for the hot climate. Ramakrishnan et al. [14] analyzed the effectiveness of *PCM* in reducing the heat stress risk during heatwave periods for the climate of Melbourne, Australia. The data showed that a combination of *PCM* and natural ventilation could reduce the duration of severe discomfort by up to 65% during summer heatwave periods. In another study, Ramakrishnan et al. [15] evaluated the effectiveness of PCM-integrated composites in improving the thermal comfort conditions inside a building located in Melbourne, Australia. The data obtained revealed that the incorporation of the *PCM* helped to reduce the indoor peak air temperature by up to 2.8 °C. Sage-Lauck and Sailor [16] conducted both experimental and numerical studies to evaluate the thermal comfort conditions of a PCM-integrated building for the climate of Oregon, USA. The authors revealed that the application of the *PCM* helped to reduce the annual overheated hours from 400 h to 200 h. Figueiredo et al. [17] experimentally and numerically studied the impact of the *PCM* on the thermal comfort inside the building with a geothermal system linked to the air conditioning system for the climate of Aviero, Portugal. The results showed that the application of the *PCM* resulted in an overheating reduction of 7.23%, showing the *PCM* efficiency of 35.49%. Gao et al. [18] studied the thermal performance of the PCM-filled hollow concrete bricks for the climate of Qingdao City, China. The results obtained revealed that the application of the optimum *PCM* reduced the attenuation rate of the inside surface temperature from 13.07% to 0.92–1.93%. Liu et al. [19] numerically studied the double glazing unit's thermal performance filled

with *PCM* in Northeast China over the winter period. The authors conducted a parametric study varying the thickness and melting temperature of the *PCM*. The results showed that varying the *PCM* thickness from 4 mm to 50 mm increased the inside surface temperature by 158.7%. The authors concluded that PCMs with melting temperatures in the range of 14–16 °C and thicknesses of 12–30 mm were optimum for Northeast China's climate. Triano-Juarez et al. [20] numerically studied the thermal performance inside a building with a PCM-integrated roof in a city in Mexico over a typical summer week. The results showed that, for a grey roof, the incorporation of a 2-cm layer of *PCM* 35 resulted in a decrease of the interior surface temperature by 6.4 °C, while, for a white roof, it was up to 15.4 °C. Dnyandip et al. [21] numerically investigated the thermal performance of a residential building roof integrated with inclined-phase change material for the climate conditions of Chennai, India. The study results showed that a PCM-integrated roof kept the ceiling temperature in the range from 25.5–27.5 °C and notably reduced the peak heat loads compared to no *PCM* case. Omari et al. [22] developed a model to study the *PCM* composite board's thermal performance in a building's walls for different seasons. The authors highlighted the importance of selecting the appropriate *PCM* melting temperature and concluded that the *PCM* composite wall boards demonstrating the best performance over the summer were the least effective in the winter season. Saffari et al. [23] tried to determine the optimum *PCM* melting temperature to decrease the energy demand of buildings for different climate conditions of the world. For the Af climate zone, the authors selected three cities: Kuala Lumpur (Malaysia), Singapore, and Puerto Barrios (Guatemala). The results demonstrated that the integration of *PCM* reduced the cooling demand of a building located in the Puerto Barrios (8% reduction); however, it was ineffective in Singapore (0.43%) and Kuala Lumpur (0.36%). Marin et al. [24] evaluated the PCM's potential to decrease the cooling and heating loads for a lightweight relocatable building. The analysis was conducted for all climate zones, including a tropical rainforest climate. Similar to the study of Saffari et al. [23], the authors found that the utilization of *PCM* under tropical climate conditions was limited and required further investigation. Lei et al. [25] investigated the impact of the *PCM* on the thermal comfort and energy consumption of a building located in the tropical climate of Singapore. The results showed that the application of the *PCM* with a melting temperature of 28 °C resulted in the largest energy savings of up to 32%. According to the authors, in the tropical climate, *PCM* cannot go through a full melting–solidification cycle due to the low diurnal temperature fluctuation and high temperatures during nighttime. However, the tropics' main advantage for *PCM* application over the other climates is the uniform weather conditions throughout the year. Thus, unlike other climates where the optimum *PCM* is selected for each season, the uniqueness of the tropical rainforest climate is the opportunity to select one optimum *PCM* for the whole year. The results of the study demonstrated that, by thoroughly selecting simulation parameters, *PCM* could significantly improve the energy consumption of the building located in the Af climate zone.

According to the literature review mentioned above, some research gaps can be noticed. Firstly, there is a lack of studies about the thermal performance of a PCM-integrated building in the tropical rainforest climate (Af climate zone). Secondly, there is a lack of studies about the impact of natural and mechanical ventilation on the thermal performance of a *PCM* building located in the Af climate zone. Therefore, this study aims to evaluate the thermal performance of buildings integrated with *PCM* and *PCM* combined with natural and mechanical ventilation located in eight cities of Af climate zone: Singapore, Kuala Lumpur, Malacca (both Malaysia), Padang (Indonesia), Davao (Philippines), Belem (Brazil), Iquitos (Peru) and Georgetown (Guyana), developing a unique methodology for selecting the *PCM* melting temperature based on the thermal comfort limits. The quantitative evaluation of the thermal performances of the PCM-integrated buildings was accomplished through a daily peak temperature drop analysis. To assess the overall impact of the *PCM* and *PCM* combined with NV/MV on the thermal performances inside the buildings, a novel indicator of the Total Temperature Drop (*TTD*), representing a sum of all decreases in the maximum

daily operative temperature throughout the year, was introduced. A comparative analysis of the PCM, PCM+NV and PCM+MV was accomplished.

2. Methodology

In this study the impact of *PCM* on the thermal performance of two-story residential buildings was investigated for different cities of Af climate zone. The analysis was accomplished using numerical simulations in Design Builder software. Figure 1 represents the detailed methodology of the study.

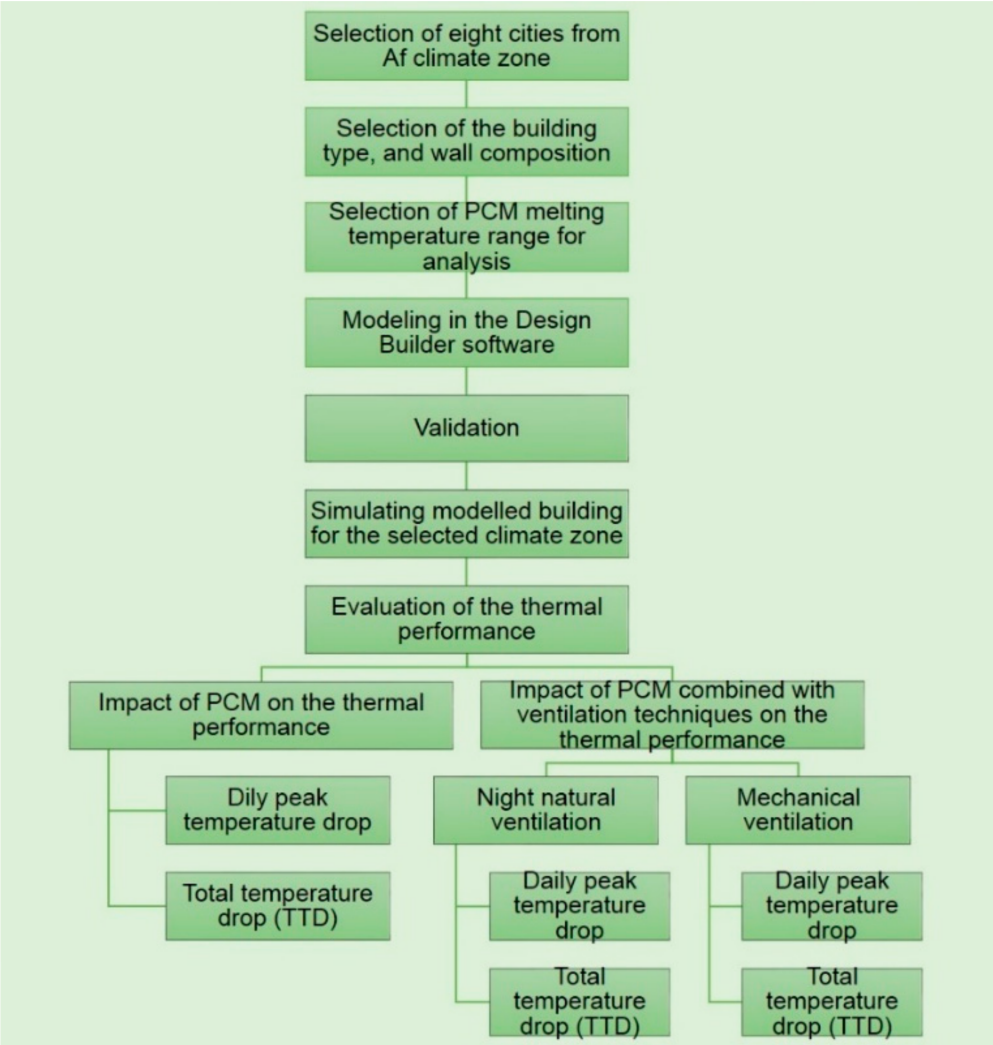

Figure 1. Methodology of the study.

2.1. Climate Characteristics

According to the Köppen-Geiger climate classification, Af represents a tropical rainforest climate with average precipitation of at least 60 mm in each month [26]. It is characterized by comparatively uniform outside air temperature throughout the year, with the average monthly air temperature exceeding 20 °C for all months [27].

For the analysis, eight cities in the Af climate zone were selected. These cities were Singapore, Kuala Lumpur, Malacca, Padang, Davao, Belem, Iquitos and Georgetown. Figure 2 illustrates the location of the Af climate zone on the world map and the eight cities selected for analysis.

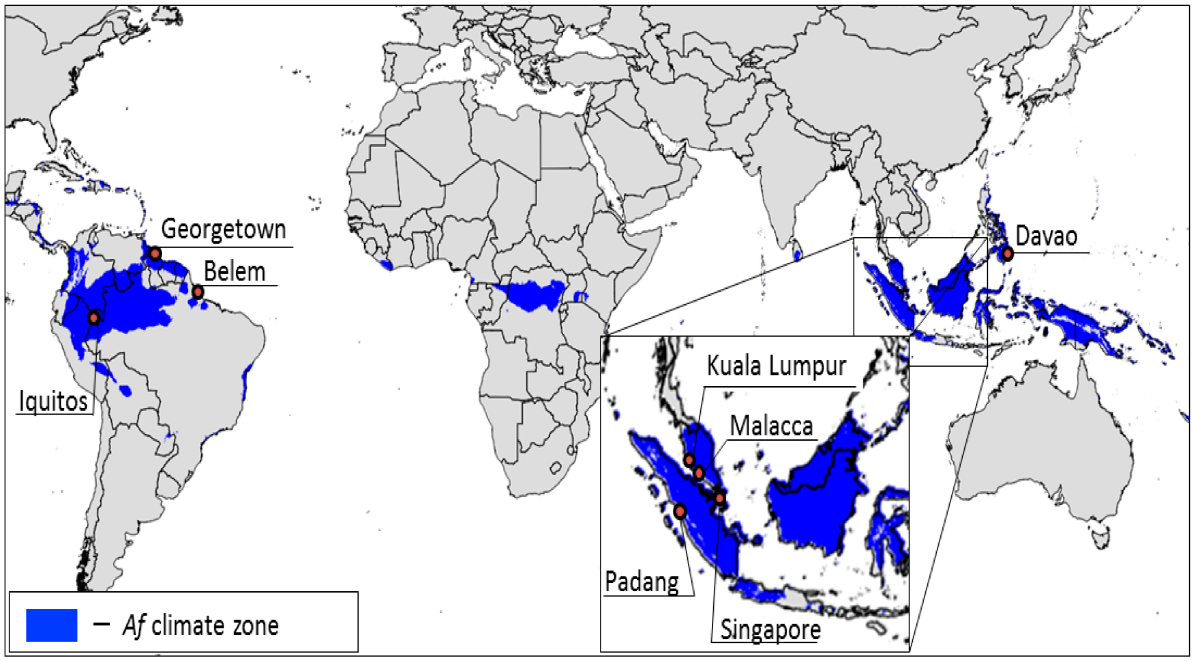

Figure 2. The territory of the tropical rainforest climate (Af) on the world map [27].

2.2. Building Description

For analysis, a two-story pitched roof residential building with a total living space area of 72 m^2 was selected. The area of each floor was 36 m^2 (9 m × 12 m). The height of each story was 3 m. The door was placed on the northern side of the building, and windows with dimensions of 2 m × 1.5 m and 2.5 m × 1.5 m were placed 0.8 m above the floor level. Figure 3 presents the details of the building envelope, while Tables 1–3 summarize the material properties of the wall roof and floor composition. Following the guidelines provided by Lei et al. [25], it was decided to place the *PCM* layer closer to the outermost layer.

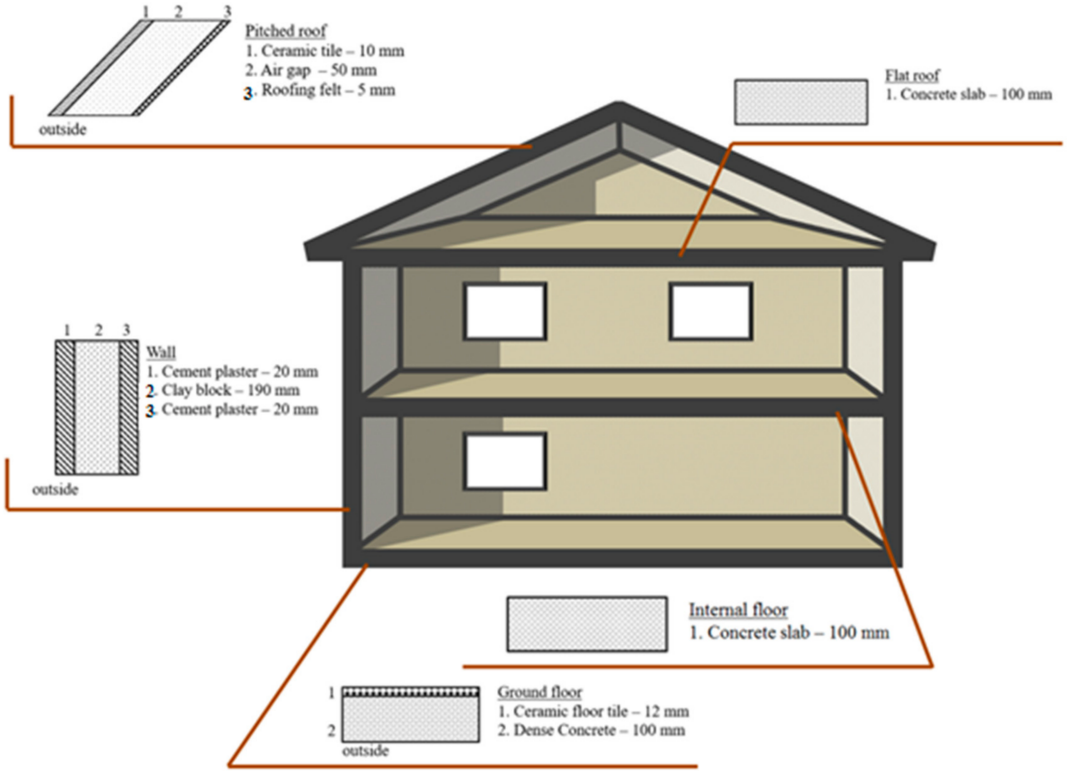

Figure 3. Schematic illustration of the building envelope.

Table 1. Thermophysical properties of the wall composition [28,29].

Material	Thickness (mm)	Thermal Conductivity (W/mK)	Density (kg/m^3)	Specific Heat (J/kgK)
Wall				
Cement plaster	20	0.8	1600	840
PCM	20	0.2	860	1970
Clay block	190	1.0	1800	920
Cement plaster	20	0.8	1600	840

Table 2. Thermophysical properties of the roof composition.

Material	Thickness (mm)	Thermal Conductivity (W/mK)	Density (kg/m^3)	Specific Heat (J/kgK)
Roof				
Ceramic tile	10	1.3	2000	840
Air gap	50	Thermal resistance (m^{2}K/W) 0.21		
PCM	20	0.2	860	1970
Roofing felt	5	0.19	960	837

Table 3. Thermophysical properties of the floors.

Material	Thickness (mm)	Thermal Conductivity (W/mK)	Density (kg/m^3)	Specific Heat (J/kgK)
Intermediate floor				
Concrete slab	100	1.13	2000	1000
Ground floor				
Dense concrete	100	1.42	2400	880
Ceramic floor tile	12	1.2	2500	640

The occupancy schedule was set from 16:00 to 8:00 h, assuming that residents were going to be at work during the daytime. During the weekends, the building was assumed to be occupied for the whole day. The infiltration rate was set to 0.5 ACH.

2.3. Thermal Comfort Limits and PCM Selection

Thermal comfort represents the conditions of human's satisfaction with the thermal environment. ASHRAE developed formulas to calculate the thermal comfort range inside a building in accordance with the climate conditions of its location. The adaptive thermal comfort approach is based on a large number of surveys conducted by the agency and allows predicting a comfortable temperature range with 80% and 90% acceptance rates [30]. In this study, the formulas of thermal comfort range with an 80% acceptance rate developed by Auliciems and Szokolay [31] were used:

$$T_{neu} = 21.5 + 0.11 \times T_{mean} \quad (1)$$

where T_{mean} stands for the average temperature for the selected period, and T_{neu} stands for the neutral temperature, which is further used to calculate the thermal comfort limits:

$$T_{max} = T_{neu} + 2\ ^{\circ}\mathrm{C} \quad (2)$$

$$T_{min} = T_{neu} - 2\ ^{\circ}\mathrm{C} \quad (3)$$

where T_{max} stands for the upper-temperature limit of the thermal comfort range, and T_{min} stands for the lower temperature limit of the thermal comfort range. For developing the thermal comfort range, the monthly temperature data was used.

Both the upper-temperature and lower-temperature limits of the thermal comfort were determined for the selected cities. However, for a comparative analysis of the cities, it was necessary to determine a thermal comfort range that would be suitable for all the cities. In this regard, it was decided to use a simple sorting algorithm to select a single comfort range for the whole tropical region (Equations (7) and (8)).

First, for each city, for each month, the minimum and maximum temperature limits were calculated. Then, for each city, one maximum and one minimum temperature limit was determined. The maximum temperature limit for the city T_{max}^{city} represents the minimum value of the monthly upper-temperature limit values. The minimum temperature limit for the city T_{min}^{city} represents the maximum value of the monthly lower-temperature limit values. The maximum temperature limit for all the cities T_{max}^{global} represents the minimum value of the maximum temperature limits determined for each city. The minimum temperature limit for all the cities T_{min}^{global} represents the maximum value of the minimum temperature limits determined for each city.

$$T_{max}^{global} = min \begin{cases} T_{max}^{city1} = min \begin{Bmatrix} T_{max}^{January} \\ \vdots \\ T_{max}^{December} \end{Bmatrix} \\ \vdots \\ T_{max}^{city8} = min \begin{Bmatrix} T_{max}^{January} \\ \vdots \\ T_{max}^{December} \end{Bmatrix} \end{cases} \quad (4)$$

$$T_{min}^{global} = max \begin{cases} T_{min}^{city\ 1} = max \begin{Bmatrix} T_{min}^{January} \\ \vdots \\ T_{min}^{December} \end{Bmatrix} \\ \vdots \\ T_{min}^{city8} = max \begin{Bmatrix} T_{min}^{January} \\ \vdots \\ T_{min}^{December} \end{Bmatrix} \end{cases} \quad (5)$$

$T_{max}^{city\ n}$ and $T_{min}^{city\ n}$ stand for maximum and minimum temperature limits of the thermal comfort of a particular city (°C), respectively; T_{max}^{global} and T_{min}^{global} stand for the global maximum and minimum temperature limits of the thermal comfort (°C), respectively. The thermal limits of each city and global thermal limits are presented in Figure 4.

As it has already been mentioned, establishing the thermal comfort limits for the model allows determining the optimum *PCM* melting temperatures. For the present study, it was found that the thermal comfort range for all cities was within the 22.68–26.37 °C range. Additionally, in the study of Lei et al. [25], the authors claimed that, for the climate of Singapore, the utilization of *PCM* 28 was the best option. Thus, considering the global thermal limits and the recommendation from reference [25], it was decided to select three PCMs at a regular interval: *PCM* 22, *PCM* 25 and *PCM* 28.

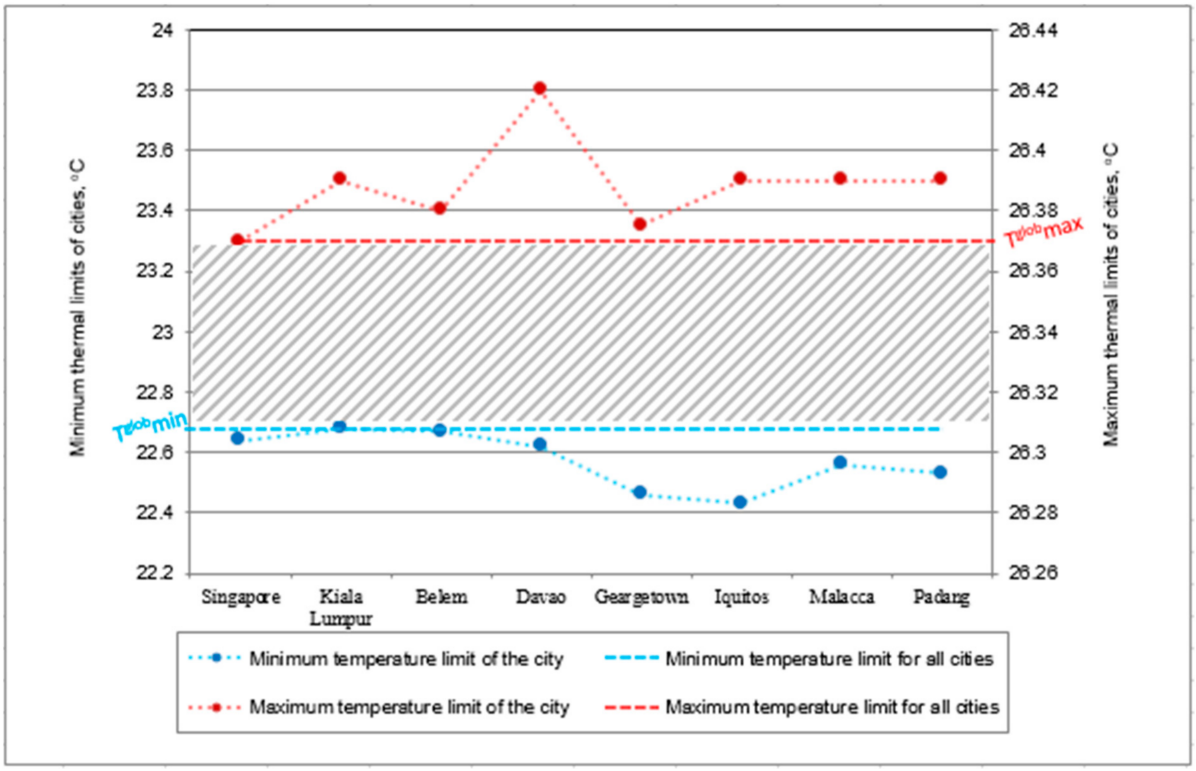

Figure 4. Minimum and maximum thermal limits for each city and global thermal comfort limits.

2.4. Characterization of PCM

To investigate the impact of the *PCM* on the thermal performance of the building, the HVAC system was switched off. *PCM* was applied in the form of a layer to the building envelope using Design Builder software. The selected type of *PCM* has a thermal conductivity of 0.2 W/mK, a density of 860 kg/m^3, specific heat of 1970 J/kgK and latent heat of 219 kJ/kg. [32]. For analysis, PCMs with the melting temperature of 22 °C, 25 °C and 28 °C were used. Each *PCM* has a phase change temperature range of 4 °C, so that, for *PCM* 22, the melting temperature ranges from 20 °C to 24 °C, for *PCM* 25, it ranges from 23 °C to 27 °C and, for *PCM* 28, it ranges from 26 °C to 30 °C. Figure 5 shows the enthalpy–temperature curves for the selected PCMs (*PCM* 22, *PCM* 25 and *PCM* 28).

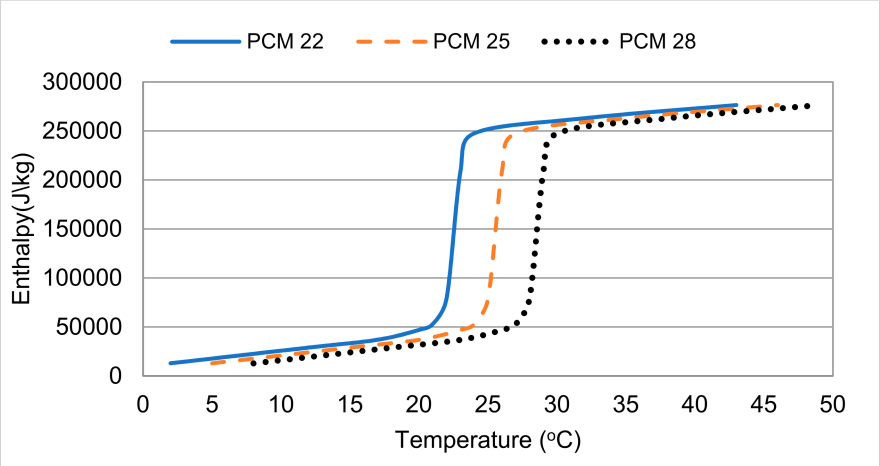

Figure 5. Enthalpy–temperature curves for *PCM* 22, *PCM* 25 and *PCM* 28.

2.5. Energy Plus and Design Builder

The numerical analysis was accomplished by means of Design Builder software using the Energy Plus simulation engine. The Energy Plus software provides a wide range of simulation options for a building's energy analysis, such as cooling, heating, lighting and ventilation load analysis [33]. In order to simulate materials with changing properties such as the PCM, a one-dimensional conduction finite-difference algorithm, also known as "CondFD", was used. The heat transfer equation based on the fully implicit scheme is as follows:

$$\frac{\rho C_p \Delta x\left(T_i^{t+1}-T_i^{t}\right)}{\Delta t}=\left[\frac{k_{i+1}^{t+1}+k_i^{t+1}}{2}\times\frac{\left(T_{i+1}^{t+1}-T_i^{t+1}\right)}{\Delta x}\right]+\left[\frac{k_{i-1}^{t+1}+k_i^{t+1}}{2}\times\frac{\left(T_{i-1}^{t+1}-T_i^{t+1}\right)}{\Delta x}\right] \quad (6)$$

where t stands for time (t+1 is a new iteration time), 1, i stands for a meshed node, (i−1 is an adjacent exterior node and i+1 is an adjacent interior node), ρ stands for the density of the selected materials (kg/m^3), C_p stands for the specific heat (kJ/kgK), T stands for the temperature of the node (K), Δt stands for the time step (s), which is selected to be 2 min, k stands for the thermal conductivity (kW/mK) and Δx stands for the nodal step (m).

The nodal step is calculated using the following formula:

$$\Delta x=\sqrt{c\cdot\alpha\cdot\Delta t} \quad (7)$$

where c stands for the space discretization constant, which is selected to be 3, and α stands for thermal diffusivity of the materials (mm^2/s).

To simulate the phase change process of the material, the CondFD algorithm is used together with the enthalpy–temperature curve of the *PCM* provided by the user. The value of equivalent specific heat for each time step is calculated in accordance with the enthalpy–temperature curve and is represented by the following formula:

$$C_P=\frac{h_i^t-h_i^{t-1}}{T_i^t-T_i^{t-1}} \quad (8)$$

where h stands for the specific enthalpy (kJ/kg).

For a detailed simulation of the *PCM* in EnergyPlus, Tabasre-Valesco et al. [34] gave some recommendations about the simulation parameters. The values of the time step should be no more than 3 min. Therefore, for this study, a time step of 2 min (Δt = 2 min) was used. The space discretization constant is recommended to be equal to 3.

2.6. Validation

In order to verify the reliability of Energy Plus in analyzing the *PCM* implementation, numerical and analytical solutions to Stephan's problem described in the study of Tabares-Velasco et al. [34] were repeated. Figure 6 summarizes the results of both the numerical and analytical solutions to Stephan's problem. According to the data presented, it can be noticed that both solutions are in good agreement. The numerical model could accurately predict the heat flux with a Root Mean Square Error of 18.1 W/m^2.

2.7. Evaluation of the Thermal Performance

Initially, the impact of the *PCM* on the thermal performance of the building was studied using the concepts of daily peak temperature drop and Total Temperature Drop (*TTD*). Thereafter, the effect of the *PCM* combined with natural and mechanical ventilation was investigated using the same thermal performance indicators: daily peak temperature drop and *TTD*.

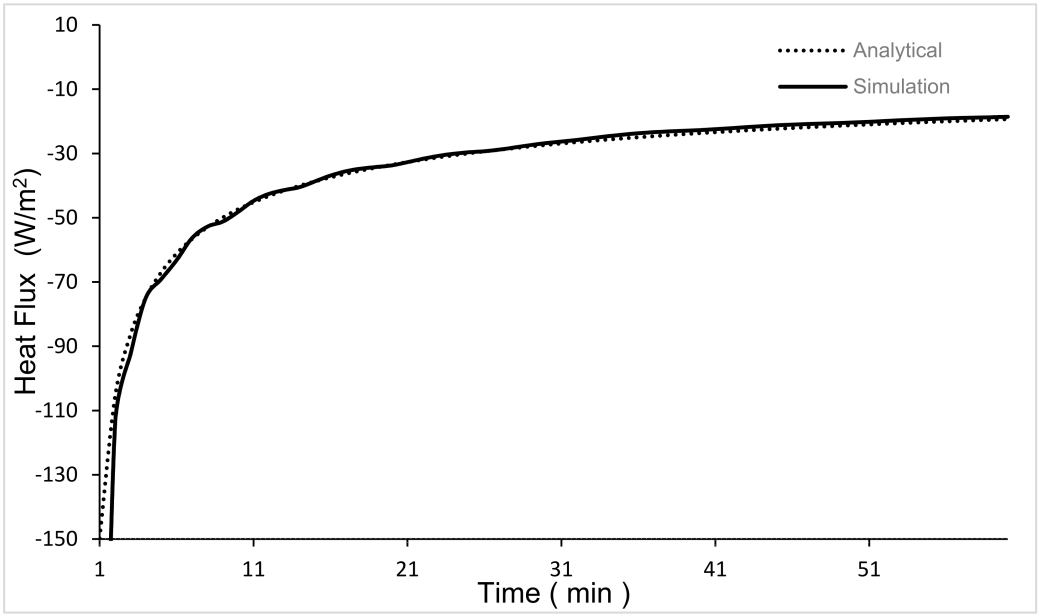

Figure 6. Analytical vs. numerical solution to Stefan's problem.

2.7.1. Daily Peak Temperature Drop

The daily peak temperature drop represents the change in the diurnal inside operative temperature with the integration of *PCM*. It can be expressed using the following formula:

$$\Delta T_{daily\ max} = T_{daily\ max\ without\ PCM} - T_{daily\ max\ with\ PCM} \quad (9)$$

where $\Delta T_{daily\ max}$ stands for the diurnal peak temperature drop, $T_{daily\ max\ without\ PCM}$ stands for the maximum daily operative temperature with no *PCM* and $T_{daily\ max\ with\ PCM}$ stands for the maximum daily operative temperature with the integration of *PCM*. For the quantitative evaluation of the thermal performance of the building over the studied period, the daily peak temperature drop values were classified into six groups, as shown below. It is important to mention that the group of negative values of the peak drop represents the cases when the application of *PCM* increased the maximum diurnal operative temperature.

$$Group\ 1: \quad \Delta T_{daily\ max} < 0\ ^{\circ}\mathrm{C}$$

$$Group\ 2: \quad 0\ ^{\circ}\mathrm{C} \leq \Delta T_{daily\ max} < 0.5\ ^{\circ}\mathrm{C}$$

$$Group\ 3: \quad 0.5\ ^{\circ}\mathrm{C} \leq \Delta T_{daily\ max} < 1\ ^{\circ}\mathrm{C}$$

$$Group\ 4: \quad 1\ ^{\circ}\mathrm{C} \leq \Delta T_{daily\ max} < 1.5\ ^{\circ}\mathrm{C}$$

$$Group\ 5: \quad 1.5\ ^{\circ}\mathrm{C} \leq \Delta T_{daily\ max} < 2\ ^{\circ}\mathrm{C}$$

$$Group\ 6: \quad 2\ ^{\circ}\mathrm{C} \leq \Delta T_{daily\ max} < 2.5\ ^{\circ}\mathrm{C}$$

2.7.2. Total Temperature Drop

The quantitative analysis of the daily peak temperature drop allows determining the number of days when the peak temperature drop fell within the specified temperature range. However, this concept does not allow evaluating the overall annual impact of the *PCM* on the thermal performance. Therefore, in order to determine the annual thermal

performance and select the best *PCM* melting temperature, a novel indicator of the Total Temperature Drop (*TTD*) was introduced. The Total Temperature Drop (Reduction) (*TTD*) represents a sum of all the maximum daily operative temperature reductions throughout the year. The *TTD* can be expressed by the following formula:

$$TTD = \sum_{1\ day}^{1\ year} (T_{daily\ max\ without\ PCM} - T_{daily\ max\ with\ PCM}) \quad (10)$$

This single value indicator shows how much the temperature can be reduced through the integration of the *PCM* to the building envelope. The higher *TTD* value stands for the better performance of the *PCM*. There are days when *PCM* integration has a negative impact on the thermal conditions inside the modeled building by increasing the indoor peak operative temperature. The negative values of the temperature change are considered in the *TTD*. The *TTD* is measured in °C.

2.8. Ventilation

In Design Builder Software, there are two methods to model natural ventilation: scheduled and calculated [35]. For the scheduled natural ventilation approach, the airflow rate, which involves the airflow coming through the outer windows and doors, is set for each zone, and the natural ventilation is activated only over the specified schedule [35]. This method is useful for the cases when the airflow rate for each zone is known; otherwise, it is less accurate. For the calculated natural ventilation, the values of the airflow rate are calculated in accordance with the dimensions of the openings and wind speed [35]. This approach is more realistic in comparison with the scheduled natural ventilation, since the airflow rate is calculated for each zone of the building based on the dimensions of the openings and outside climate conditions. Therefore, for this study, the calculated natural ventilation approach was applied. Since the effectiveness of the calculated natural ventilation method directly depends on the outside weather conditions, it is worth mentioning that, sometimes, NV may negatively affect the inside thermal conditions. For example, in the cases when the outside air temperature is hotter than the inside air temperature, the application of natural ventilation may result in overheating of the room. Therefore, to avoid the heat flow from the outside environment to the building, natural ventilation operated only when the outside temperature was 2 °C (or more) lower than the inside temperature (T_{in}–$T_{out} \geq 2$ °C). Natural ventilation was applied over the nighttime from 19:00 to 07:00 h. The opening area was set to 5% of the window area.

Mechanical ventilation is a process of circulating fresh air inside the building using ducts and fans. In Design Builder software, mechanical ventilation is modeled by setting the value of the constant airflow rate and operation schedule [36]. For this study, the airflow rate of 4 ACH was used. The working hours of mechanical ventilation were set in accordance with the occupancy schedule from 16:00 to 08:00 h to prevent the flow of the hot air from the outside environment to the building in periods of heatwave events. This option involves the condition stating that, for initiating the mechanical ventilation process, the indoor air temperature should be at least 2 °C lower than the outside air temperature. In case the condition was not satisfied, the mechanical ventilation would be switched off. Ventilation models used for the simulations are presented in the schematic drawing below (Figure 7).

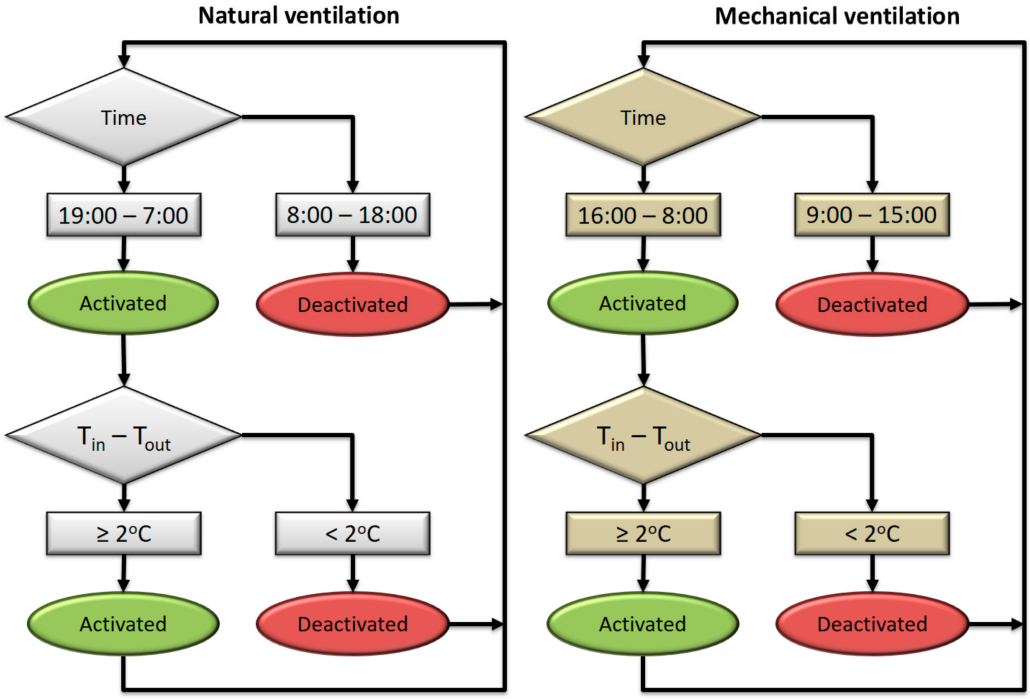

Figure 7. Schematic representation of ventilation of the modeled building.

3. Results

3.1. Impact of PCM the Thermal Performance

In this section, the results of the evaluation of the impact of the *PCM* on the daily peak temperature drop and Total Temperature Drop (*TTD*) for all eight cities are presented. Figure 8 summarizes the results of the maximum temperature drop and *TTD* values for all the cities. According to the data presented, it is seen that, in all the cities, the PCMs decreased the peak operative temperature for most of the days. However, in all the cities, *PCM* 28 showed a more efficient performance, resulting in a higher number of days when the maximum temperature was reduced by the value in the range from 1.5 °C to 2.5 °C. Additionally, from Figure 8, it is seen that, in all the cities, compared with *PCM* 22 and *PCM* 25, the usage of *PCM* 28 resulted in a higher *TTD* value of up to 356 °C per year. The superiority of *PCM* 28 is related to the region's hot climate conditions, which are more suitable for *PCM* 28 to complete the phase change cycle. Since the temperature reached high values even at nighttime, the *PCM* with a higher melting temperature could solidify more frequently in comparison with PCMs with lower melting temperatures.

The results presented in Figure 8 demonstrate that the utilization of *PCM* increases the maximum temperature of the day. According to the data, in the majority of the cities, a peak temperature rise ($\Delta T_{daily\ max} < 0$ °C) was observed during less than 5% of the studied period. However, in Iquitos and Georgetown, the application of the *PCM* resulted in higher values of temperature rise ($\Delta T_{daily\ max} < 0$ °C). For Iquitos, the integration of *PCM* 28 to the building envelope increased the daily maximum temperature for 25 days, which is about 7% of the year, and in Georgetown, it was increased for 67 days (18%).

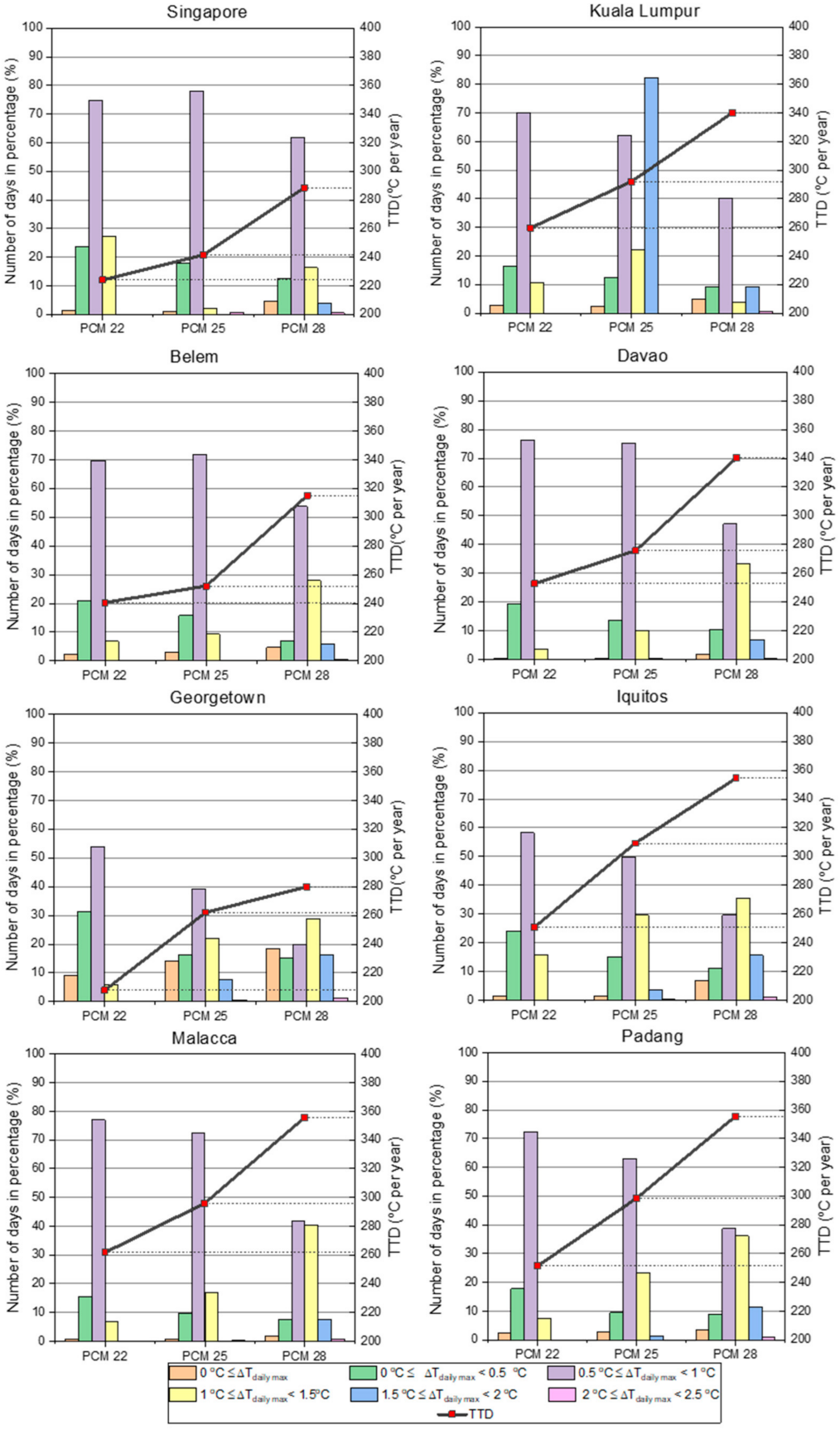

Figure 8. Impact of *PCM* 22, *PCM* 25 and *PCM* 28 on the maximum daily temperature drop and *TTD* values for all the cities.

To explain this difference in results, two separate days with the positive and negative impacts of the *PCM* on the peak temperature were examined. The days with a positive impact of the *PCM* were termed as "positive days", whereas days with a negative impact of the *PCM* were termed as "negative days". The values of outside air temperature and the hourly inside operative temperature for the cases when the building was without *PCM* and when it was with *PCM* 28 during positive and negative days on the peak operative temperature for the city of Georgetown are summarized in Figure 9. According to the results obtained, during the positive day, the inside operative temperature fluctuation was in the range of 26–28.76 °C, while the outside air temperature varied from 23.5 °C to 29 °C. On a negative day, the inside operative temperature fluctuation was from 24 °C to 25.18 °C, whereas the outside air temperature was from 23.2 °C to 26 °C. Thus, it was seen that, during the day, with a positive impact of the PCM, the outside temperature conditions and, as a result, indoor thermal conditions were favorable for *PCM* 28 to complete its melting–solidification cycle. In contrast, during a negative day, the outside temperature and inside temperature were not favorable for the *PCM* 28 to completely go through the melting–solidification cycle. Therefore, most of the time, *PCM* 28 was in a solid state, serving as an additional thermal mass applied to the building envelope. The additional thermal mass resulted in the heating of the building during the daytime and the inability to release the heat over the nighttime. The above statement explains the occasional negative effect of *PCM* on the daily maximum temperature. The fact that the cities of Iquitos and Georgetown had the highest percentages of negative days in comparison with the other cities is related to the climate conditions of these two cities. According to the weather data, these two cities are characterized by comparatively lower average outside temperatures in comparison with the other cities. For Iquitos and Georgetown, the average outside temperatures for the whole year were 25.68 °C and 26.08 °C, respectively, whereas the average temperatures for the rest of the cities were in the range of 26.7–27.8 °C. This means that, in general, in these cities (Iquitos and Georgetown), the ambient temperatures throughout the day were low. Consequently, the number of days when *PCM* could go through the melting–solidification cycle was less in comparison with the other cities. This statement explains why these cities were characterized by the highest number of days with a negative performance of *PCM* 28.

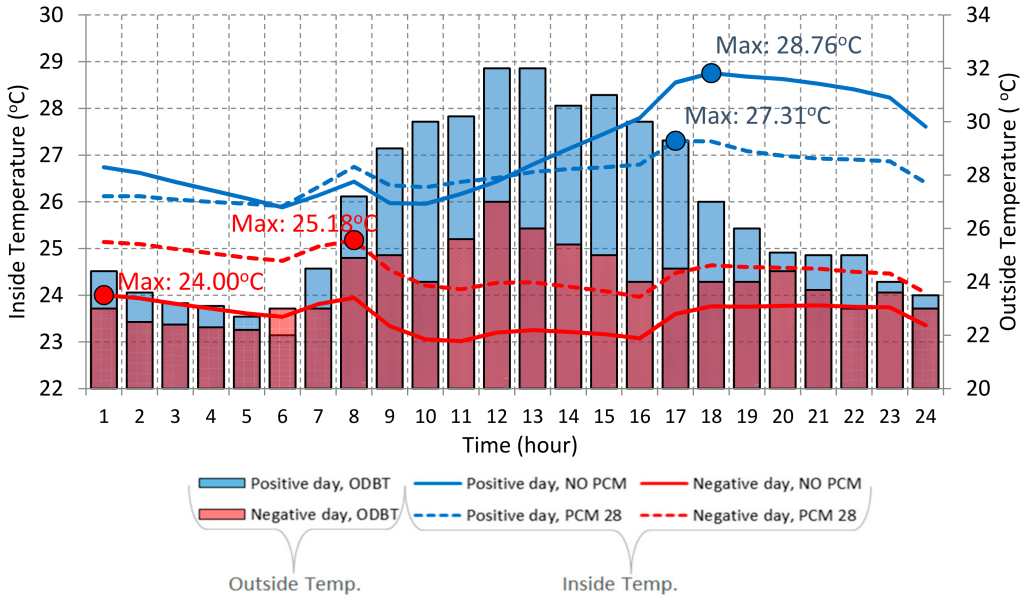

Figure 9. Inside operative temperature and outside temperature for positive and negative days for the city of Georgetown.

3.2. Impact of PCM Combined with Ventilation Techniques on the Thermal Performance

Several studies [8–11,14,37–39] have shown that the application of ventilation over the nighttime could significantly enhance the performance of the *PCM* in terms of improving the thermal comfort inside the building. Since, in the previous sections, *PCM* 28 showed the most efficient performance, it was selected for investigation of the combined effect of the *PCM* and night ventilation. In this section, both natural ventilation (NV) and mechanical ventilation (MV) were considered. The results of the "*PCM* 28" case were compared against the "*PCM* 28 + NV/MV" cases.

3.2.1. Natural Ventilation

Figure 10 and Table 4 summarize the maximum daily temperature drop and *TTD* values for all the cities for *PCM* 28 and *PCM* 28 + NV cases. According to the data presented, it can be observed that applying natural ventilation at night had a positive effect on the values of peak temperature drop and, consequently, on the values of *TTD* of all eight cities. The incorporation of ventilation for the night period lowered the inside heat, which consequently facilitated the solidification of the *PCM* layer. In all the cases, the application of natural ventilation during the nighttime increased the *TTD* values by up to 15% in comparison with the no ventilation case. In Padang and Iquitos, the *TTD* values were 7.18% and 8.85%, respectively, which were relatively lower when compared with the other cities. The lower values of the rise in *TTD* for these two cities can be explained by the climate conditions of the cities. It is worth mentioning that natural ventilation heavily depends on wind speed, which itself depends on local climate conditions [9]. To support the results, the monthly average wind speed data for all the cities was considered (Table 5). Comparing the effectiveness of natural ventilation with the local wind speed, the direct relationship between these two can be noticed. The lowest average wind speed values belong to Padang and Iquitos, where the lowest increase in the *TTD* values were obtained.

Table 4. *TTD* values for all the cities for the *PCM* 28 and *PCM* 28 + NV cases.

City	*PCM* 28 (°C per Year)	*PCM* 28 + NV (°C per Year)	Increase (%)
Singapore	288.43	326.96	13.36
Kuala Lumpur	339.90	383.44	12.81
Malacca	355.82	401.87	12.94
Padang	355.52	381.04	7.18
Belem	315.06	361.12	14.62
Davao	340.58	385.93	13.32
Georgetown	279.86	323.88	15.73
Iquitos	354.41	385.76	8.85

Several studies investigated the effect of natural ventilation on the performance of the *PCM*. For example, Jamil et al. [11] integrated nighttime ventilation along with *PCM* for the climate of Melbourne. The natural ventilation scheduled from 19:00 to 7:00 h considerably reduced the inside air temperature, including the diurnal maximum temperature. The authors reported 1.5–2 °C, 1–1.5 °C, 0.5–1 °C and 0.5–0 °C peak temperature reductions for 16%, 19%, 16% and 45% of the days, respectively. Liu et al. [39] compared different strategies of introducing *PCM* and NV to a building to decrease the thermal discomfort inside the buildings located in 10 cities of Western China over the hot season. Comparing the cases of "without *PCM* and NV", "with PCM", "with NV" and "with *PCM* and NV", they concluded that coupling *PCM* with NV was the best strategy for the hot climate. The usage of *PCM* + NV significantly reduced the intensity of the thermal discomfort and the number of discomfort hours for all the cities. The results showed that the combination of *PCM* and natural ventilation reduced the inside temperature by up to 2 °C. Thus, based on the studies about the combined application of *PCM* and natural ventilation mentioned

above, it can be concluded that the effectiveness of natural ventilation directly depends on the local weather conditions.

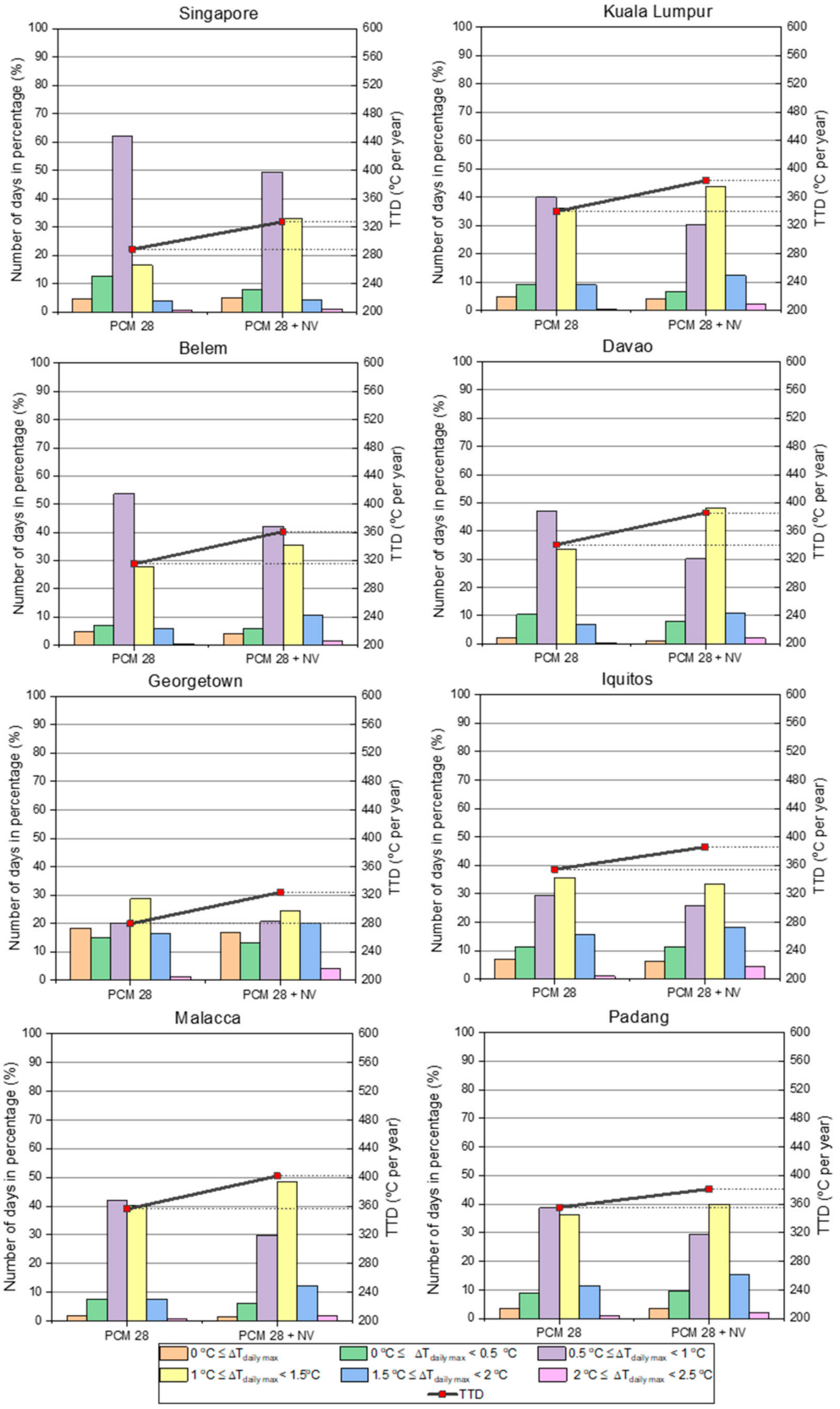

Figure 10. Impact of *PCM* 28 and *PCM* 28 + NV on the maximum daily temperature drop and *TTD* values for all the cities.

Table 5. Average monthly wind speed data and *TTD* increase values for all the cities.

City	Padang	Iquitos	Kuala L	Malacca	Davao	Belem	Singapore	Georgetown
	Average Monthly Wind Speed (m/s)							
January	0.93	1.54	1.30	2.28	2.75	1.57	2.40	2.49
February	1.34	1.45	1.72	2.57	2.99	2.45	3.78	2.72
March	0.88	2.86	1.65	2.45	2.58	2.41	1.76	3.37
April	1.24	0.66	1.41	1.00	2.05	2.32	1.36	2.63
May	0.79	0.37	1.79	1.30	1.65	2.39	1.64	2.73
June	1.06	0.70	1.50	1.34	1.77	2.51	1.71	2.21
July	1.30	0.84	1.98	1.08	1.02	1.50	2.65	1.55
August	1.15	0.75	1.68	1.21	1.76	1.92	2.91	1.58
September	0.98	0.85	1.83	1.27	1.33	1.73	1.71	1.98
October	0.81	1.12	1.69	1.80	1.31	3.30	1.59	2.34
November	0.71	0.48	1.30	2.17	1.08	2.01	1.92	2.34
December	0.72	1.35	1.47	1.49	1.97	1.52	3.74	1.95
Annual Average	**0.99**	**1.08**	**1.61**	**1.66**	**1.86**	**2.14**	**2.26**	**2.32**
***TTD* increase (%)**	**7.18**	**8.85**	**12.81**	**12.94**	**13.32**	**14.62**	**13.36**	**15.73**

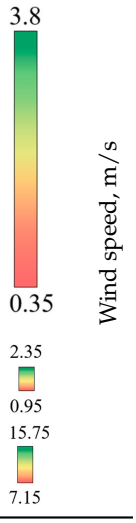

* Values of the wind speed colored in a gradient pattern, with the red being lowest and the green being highest (for visualization purposes).

Based on the results presented in this section, it can be concluded that the incorporation of nighttime NV can have a positive effect on the *PCM* performance. The addition of airflow was able to reduce the inside heat and the maximum daily temperature. Moreover, it was found that the effectiveness of NV is directly related to the weather conditions at which the model is simulated. Finally, Table 3 shows that, in all the cities, most of the time, the wind speed was lower than 3 m/s, which might consequently result in a low airflow rate. Therefore, the application of mechanical ventilation characterized by a controlled airflow rate was considered in the following section.

3.2.2. Mechanical Ventilation

Figure 11 and Table 6 demonstrate the results of the impact of *PCM* combined with mechanical ventilation on the peak temperature drop and *TTD* value. Similar to natural ventilation, the application of mechanical ventilation resulted in increased peak temperature drop values in all the cities. For most cities, the *TTD* values were around 400–500 °C per year, with slightly higher results in Iquitos (513.62 °C per year) and Padang (511.27 °C per year) and comparatively lower results in Georgetown (381.68 °C per year). The improvement of the *TTD* values due to the controlled airflow rate was in the range of 26–45% in comparison with the PCM-only case. Compared with *PCM* + NV, the application of *PCM* together with MV increased the *TTD* values in the range of 16–37%. Thus, the application of forced ventilation can noticeably decrease the maximum temperature inside the building.

Table 6. *TTD* values for all the cities for the *PCM* 28 and *PCM* 28 + MV cases, and the difference in the *TTD* increase between *PCM* 28 + NV and *PCM* 28 + MV.

City	*PCM* 28 (°C per Year)	*PCM* 28+MV (°C per Year)	Increase (%)	Difference between NV and MV (%)
Singapore	288.43	413.98	43.53	30.17
Kuala Lumpur	339.90	434.75	27.90	15.09
Malacca	355.82	449.03	26.20	13.26
Padang	355.52	511.27	43.81	36.63
Belem	315.06	431.09	36.83	22.21
Davao	340.58	484.39	42.23	28.91
Georgetown	279.86	381.68	36.38	20.65
Iquitos	354.41	513.62	44.92	36.07

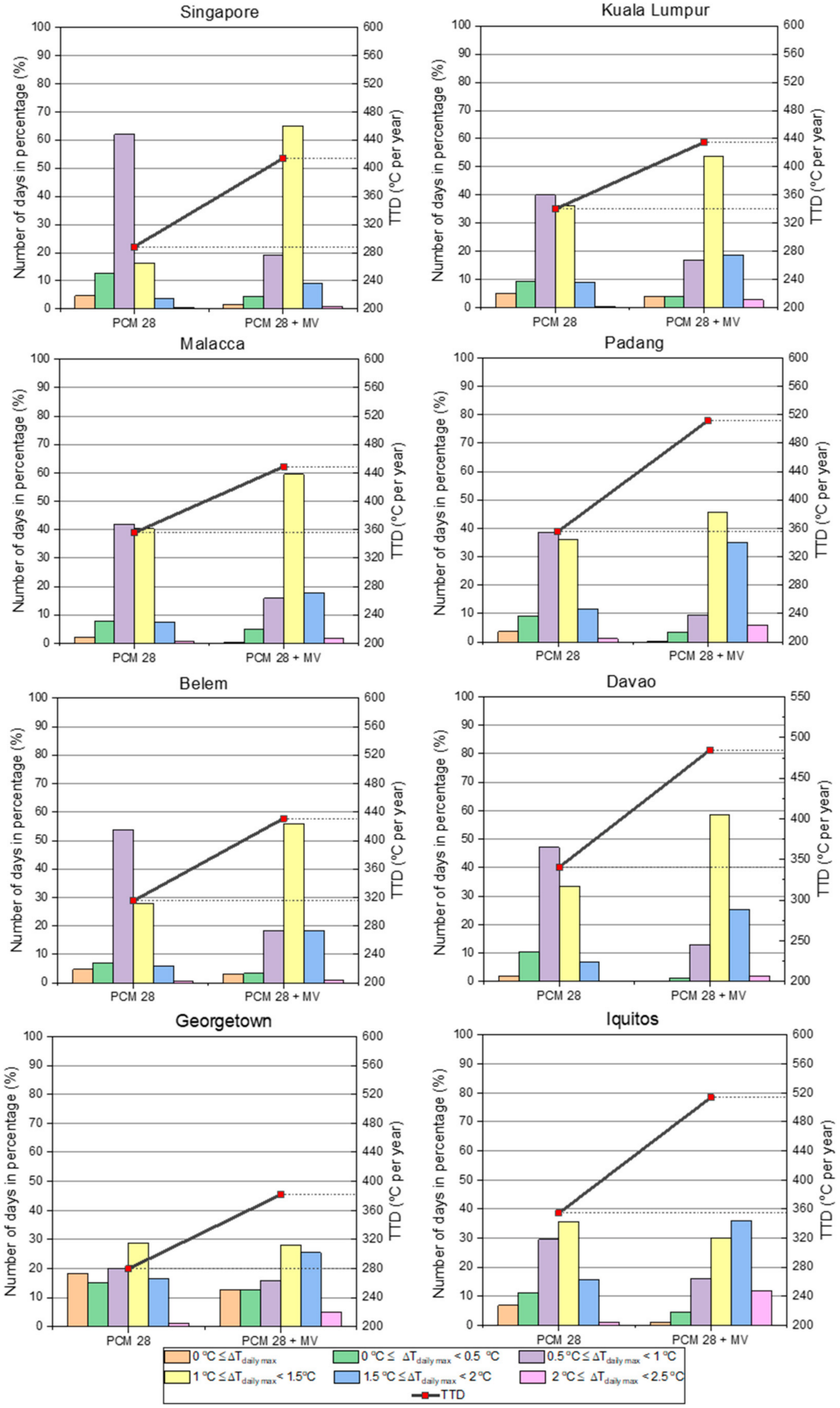

Figure 11. Maximum daily temperature drop and *TTD* values for all the cities integrating *PCM* 28 and *PCM* 28 + MV.

Additionally, MV significantly reduced the number of "negative days" in comparison with NV. Table 7 demonstrates the number of "negative days" for the *PCM* 28, *PCM* 28 + NV and *PCM* 28 + MV cases. Based on the results obtained, the following conclusions can be drawn. Firstly, the integration of NV helped to decrease the number of "negative days" only in a few cases. Secondly, the integration of MV had a substantial impact on the number of "negative days". The application of MV considerably reduced the number of negative days for all the cities except for Kuala Lumpur.

Table 7. The number of "negative days".

City	*PCM* 28	*PCM* 28 + NV	Reduction (%)	*PCM* 28 + MV	Reduction (%)	Difference between NV and MV (%)
Singapore	17	16	5.88	6	64.71	58.82
Kuala Lumpur	18	15	16.67	14	22.22	5.56
Malacca	7	5	28.57	1	85.71	57.14
Padang	13	13	0.00	1	92.31	92.31
Belem	17	15	11.76	11	35.29	23.53
Davao	7	4	42.86	1	85.71	42.86
Georgetown	67	62	7.46	46	31.34	23.88
Iquitos	25	23	8.00	4	84.00	76.00

For a more detailed analysis of the effect of MV on the thermal conditions inside the building, it was decided to conduct a one-day analysis on an hourly basis. Moreover, to examine the difference between MV and NV, the case of *PCM* + NV was added to the graph. As an example, the city of Georgetown was selected for analysis. Figure 12 summarizes the results of the outside dry bulb temperature (ODBT) and inside temperature of the building for no the PCM, *PCM* 28, *PCM* 28 + NV and *PCM* 28 + MV cases. According to the data, the integration of *PCM* 28 negatively affected the inside thermal conditions, as its incorporation increased the inside temperature for the whole day. In this regard, the selected day can be considered as the "negative day". Additionally, the graph demonstrates hours when ventilation was activated. Although the schedules of MV and NV were from 16:00 to 8:00 h and from 19:00 to 7:00 h, respectively, the activation time of both ventilations on this day was from 1:00 to 7:00 h and from 21:00 to 24:00 h. This was due to the operational limits of both ventilations, which prevent overheating of the room by maintaining the condition of Tin—Tout $\geq$ 2 °C. In Figure 12, the working hours of the ventilations are colored in green. It is seen that, in comparison with the *PCM* 28 case, the usage of ventilation together with *PCM* 28 was more efficient in reducing the heat inside the building. During the nighttime period, from 01:00 to 7:00 h, both natural and mechanical ventilation actively decreased the inside temperature. However, since the airflow rate of NV was limited, its effectiveness was significantly lower in comparison with MV. During the daytime, both ventilations were switched off. Nevertheless, since the building was cooled during the night, the inside temperature for these cases was lower in comparison with the *PCM* 28 case. The ventilation after 21:00 h significantly reduced the inside temperature of the building during the nighttime period. The example showed the effectiveness of ventilation in decreasing the inside temperature of the building. Despite that both natural and mechanical ventilation reduced the inside temperature, MV demonstrated its superiority over NV, as it used a controlled airflow rate. It is important to note that, for *PCM* 28, the peak daily temperature was 26.18 °C, which is 0.33 °C higher than for the no *PCM* (25.85 °C) case. The integration of NV helped result in the maximum temperature of 26.05 °C, but it was still higher than for the no *PCM* (25.85 °C) case, and the day was still considered as the "negative day". However, the application of MV reduced the daily peak temperature to 25.73 °C, which was slightly lower than for the no *PCM* (25.85 °C) case. In this regard, *PCM* 28 + MV could change this particular "negative day" to a positive one. Although the integration of NV improved the thermal performance in terms of the maximum daily temperature, mostly, it was not enough to change "negative days" into positive ones.

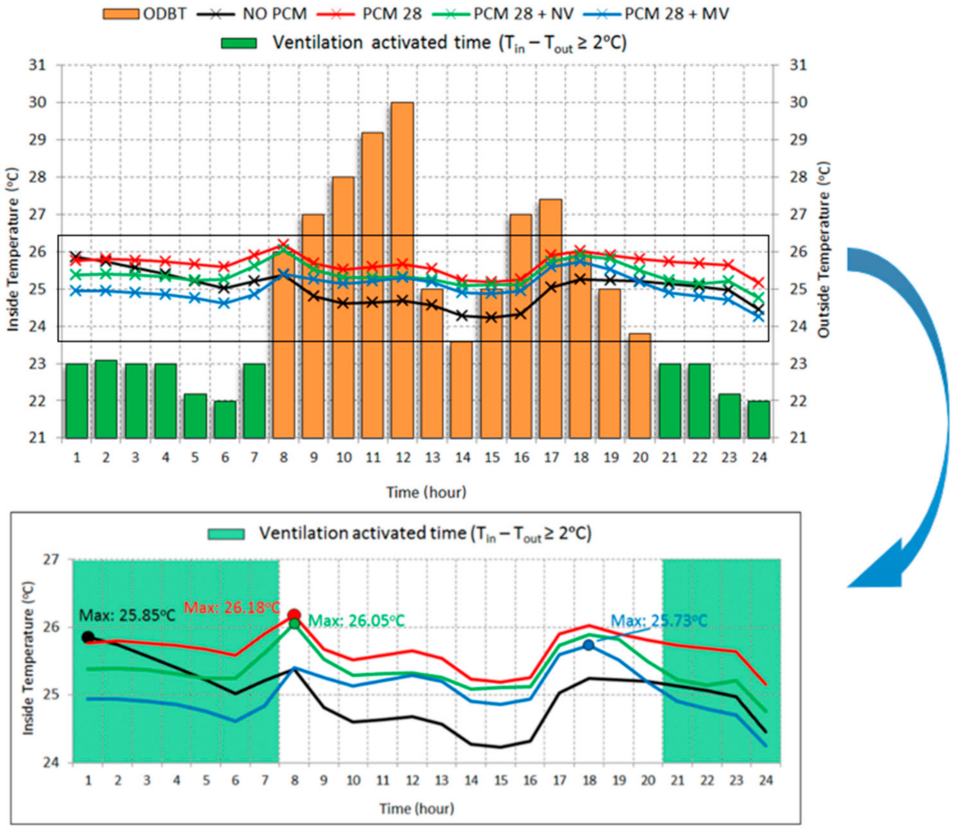

Figure 12. One-day analysis of the inside operative temperature of the building for the no PCM, *PCM* 28, *PCM* 28 + NV and *PCM* 28 + MV cases for the city of Georgetown.

4. Conclusions and Recommendations

This study investigated the impact of the *PCM* on the thermal performance of a building located in eight cities of the Af climate zone: Singapore, Kuala Lumpur, Malacca (both Malaysia), Padang (Indonesia), Davao (Philippines), Belem (Brazil), Iquitos (Peru) and Georgetown (Guyana). The thermal performance of the building integrated with *PCM* was investigated through the daily peak temperature drop and novel indicator of the Total Temperature Drop (*TTD*). The thermal comfort limits were set for the whole climate zone using a simplified sorting algorithm. Additionally, the potential of nighttime natural and mechanical ventilation to enhance the performance of the *PCM* in improving the thermal conditions inside the building was analyzed. The main findings of the study are summarized below.

- In all cities, compared to *PCM* 22 and *PCM* 25, *PCM* 28 showed the most efficient performance in terms of the daily peak temperature drop and Total Temperature Drop. Thus, it can be considered as optimum for the whole Af climate zone. The usage of *PCM* 28 resulted in the *TTD* values of all the cities ranging from 279 °C per year to 356 °C per year.
- Introducing natural ventilation for the nighttime period helped to increase the *TTD* values by up to 15%. In Padang and Iquitos, the integration of NV resulted in *TTD* values of 8.85% and 7.18%, respectively. The less effective performance of NV in these two cities was related to the lower wind speed values. The results suggested that the effectiveness of NV is directly dependent on the wind speed.
- Introducing mechanical ventilation helped to increase the *TTD* values for all the cities by 16–45%. It demonstrated that the forced airflow rate could be beneficial for the tropical climate. A comparison between the two ventilation types demonstrated the superiority of MV over NV, as the second one heavily depends on the weather conditions of the location.

- Overall, *PCM* 28 combined with MV can be successfully used to improve the thermal performance of a building located in the Af climate zone.
- For future studies, it is recommended to investigate the impact of the outside relative humidity on the thermal comfort conditions inside a PCM-integrated building located in the Af climate zone. Additionally, the impact of the window opening area on the thermal performance of a building in the Af climate zone should be evaluated.

Author Contributions: Conceptualization, S.A.M. and A.S.; Funding acquisition, S.A.M. and J.K.; Investigation, A.S. and I.A., Methodology, A.S. and S.A.M.; Formal analysis, A.S.; Software, A.S.; Visualization, A.S.; Writing—original draft, A.S. and Writing—reviewing and editing, I.A., S.A.M. and J.K. All authors have read and agreed to the published version of the manuscript.

Funding: This research was supported by Nazarbayev University Faculty development competitive research grants numbers 021220FD0651 and NU Research grant number SOE2017003.

Institutional Review Board Statement: Not applicable.

Informed Consent Statement: Not applicable.

Conflicts of Interest: The authors declare no conflict of interest.

References

1. IEA Fossil Fuel Energy Consumption. Available online: https://data.worldbank.org/indicator/EG.USE.COMM.FO.ZS (accessed on 24 May 2020).
2. IEA Energy Efficiency: Buildings. Available online: https://www.iea.org/topics/energyefficiency/buildings/ (accessed on 15 August 2019).
3. Du, K.; Calautit, J.; Wang, Z.; Wu, Y.; Liu, H. A review of the applications of phase change materials in cooling, heating and power generation in different temperature ranges. *Appl. Energy* **2018**, *220*, 242–273. [CrossRef]
4. Oró, E.; de Gracia, A.; Castell, A.; Farid, M.M.; Cabeza, L.F. Review on phase change materials (PCMs) for cold thermal energy storage applications. *Appl. Energy* **2012**, *99*, 513–533. [CrossRef]
5. Kasaeian, A.; Bahrami, L.; Pourfayaz, F.; Khodabandeh, E.; Yan, W.M. Experimental studies on the applications of PCMs and nano-PCMs in buildings: A critical review. *Energy Build.* **2017**, *154*, 96–112. [CrossRef]
6. Rao, V.V.; Parameshwaran, R.; Ram, V.V. PCM-mortar based construction materials for energy efficient buildings: A review on research trends. *Energy Build.* **2018**, *158*, 95–122. [CrossRef]
7. Zhou, G.; Yang, Y.; Wang, X.; Zhou, S. Numerical analysis of effect of shape-stabilized phase change material plates in a building combined with night ventilation. *Appl. Energy* **2009**, *86*, 52–59. [CrossRef]
8. Alam, M.; Sanjayan, J.; Zou, P.X.W.; Ramakrishnan, S.; Wilson, J. Evaluating the passive and free cooling application methods of phase change materials in residential buildings: A comparative study. *Energy Build.* **2017**, *148*, 238–256. [CrossRef]
9. Zhang, Y.; Cui, H.; Tang, W. Effect of Summer Ventilation on the Thermal Performance and Energy Efficiency of Buildings Utilizing Phase Change Materials. *Energies* **2017**, *10*, 1214. [CrossRef]
10. Evola, G.; Marletta, L.; Sicurella, F. A methodology for investigating the effectiveness of *PCM* wallboards for summer thermal comfort in buildings. *Energy Build.* **2014**, *70*, 480–489. [CrossRef]
11. Jamil, H.; Alam, M.; Sanjayan, J.; Wilson, J. Investigation of *PCM* as retrofitting option to enhance occupant thermal comfort in a modern residential building. *Energy Build.* **2016**, *133*, 217–229. [CrossRef]
12. Li, D.; Zheng, Y.; Liu, C.; Wu, G. Numerical analysis on thermal performance of roof contained *PCM* of a single residential building. *Energy Convers. Manag.* **2015**, *100*, 147–156. [CrossRef]
13. Ahangari, M.; Maerefat, M. An innovative *PCM* system for thermal comfort improvement and energy demand reduction in building under different climate conditions. *Sustain. Cities Soc.* **2019**, *44*, 120–129. [CrossRef]
14. Ramakrishnan, S.; Wang, X.; Sanjayan, J.; Wilson, J. Thermal performance of buildings integrated with phase change materials to reduce heat stress risks during extreme heatwave events. *Appl. Energy* **2017**, *194*, 410–421. [CrossRef]
15. Ramakrishnan, S.; Wang, X.; Sanjayan, J.; Wilson, J. Thermal performance assessment of phase change material integrated cementitious composites in buildings: Experimental and numerical approach. *Appl. Energy* **2017**, *207*, 654–664. [CrossRef]
16. Sage-Lauck, J.S.; Sailor, D.J. Evaluation of phase change materials for improving thermal comfort in a super-insulated residential building. *Energy Build.* **2014**, *79*, 32–40. [CrossRef]
17. Figueiredo, A.; Vicente, R.; Lapa, J.; Cardoso, C.; Rodrigues, F.; Kämpf, J. Indoor thermal comfort assessment using different constructive solutions incorporating. *PCM. Appl. Energy* **2017**, *208*, 1208–1221. [CrossRef]
18. Gao, Y.; He, F.; Meng, X.; Wang, Z.; Zhang, M.; Yu, H.; Gao, W. Thermal behavior analysis of hollow bricks filled with phase-change material (PCM). *J. Build. Eng.* **2020**, *31*, 101447. [CrossRef]
19. Liu, C.; Wu, Y.; Li, D.; Zhou, Y.; Wang, Z.; Liu, X. Effect of *PCM* thickness and melting temperature on thermal performance of double glazing units. *J. Build. Eng.* **2017**, *11*, 87–95. [CrossRef]

20. Triano-Juárez, J.; Macias-Melo, E.V.; Hernández-Pérez, I.; Aguilar-Castro, K.M.; Xamán, J. Thermal behavior of a phase change material in a building roof with and without reflective coating in a warm humid zone. *J. Build. Eng.* **2020**, *32*, 101648. [CrossRef]
21. Bhamare, D.K.; Rathod, M.K.; Banerjee, J. Numerical model for evaluating thermal performance of residential building roof integrated with inclined phase change material (PCM) layer. *J. Build. Eng.* **2020**, *28*, 101018. [CrossRef]
22. El Omari, K.; Le Guer, Y.; Bruel, P. Analysis of micro-dispersed PCM-composite boards behavior in a building's wall for different seasons. *J. Build. Eng.* **2016**, *7*, 361–371. [CrossRef]
23. Saffari, M.; de Gracia, A.; Fernández, C.; Cabeza, L.F. Simulation-based optimization of *PCM* melting temperature to improve the energy performance in buildings. *Appl. Energy* **2017**, *202*, 420–434. [CrossRef]
24. Marin, P.; Saffari, M.; de Gracia, A.; Zhu, X.; Farid, M.M.; Cabeza, L.F.; Ushak, S. Energy savings due to the use of *PCM* for relocatable lightweight buildings passive heating and cooling in different weather conditions. *Energy Build.* **2016**, *129*, 274–283. [CrossRef]
25. Lei, J.; Yang, J.; Yang, E.H. Energy performance of building envelopes integrated with phase change materials for cooling load reduction in tropical Singapore. *Appl. Energy* **2016**, *162*, 207–217. [CrossRef]
26. Mindat.org. Tropical rainforest climate. Available online: https://www.mindat.org/climate-Af.html (accessed on 1 April 2021).
27. Wikipedia Contributors. Tropical Rainforest Climate. Available online: https://en.wikipedia.org/w/index.php?title=Tropical_rainforest_climate&oldid=948667960 (accessed on 2 April 2020).
28. Moreno, A.C.R.; De Morais, I.S.; De Souza, R.G. Thermal Performance of Social Housing—A Study Based on Brazilian Regulations. *Energy Procedia* **2017**, *111*, 111–120. [CrossRef]
29. Sadeghifam, A.N.; Zahraee, S.M.; Meynagh, M.M.; Kiani, I. Combined use of design of experiment and dynamic building simulation in assessment of energy efficiency in tropical residential buildings. *Energy Build.* **2015**, *86*, 525–533. [CrossRef]
30. AHSRAE-55-2010 ASHRAE STANDARD. *Thermal Environment Conditions for Human Occupancy*; American Society of Heating, Refrigerating and Air-Conditioning Engineers: Atlanta, GA, USA, 2010.
31. Auliciems, A.; Szokolay, S.V. *Thermal Comfort*, 2nd ed.; Passive and Low Energy Architecture International in association with Department of Architecture, The University of Queensland: Brisbane, Australia, 2007.
32. Alam, M.; Jamil, H.; Sanjayan, J.; Wilson, J. Energy saving potential of phase change materials in major Australian cities. *Energy Build.* **2014**, *78*, 192–201. [CrossRef]
33. EnergyPlus. Available online: https://www.energyplus.net/ (accessed on 17 April 2020).
34. Tabares-Velasco, P.C.; Christensen, C.; Bianchi, M. Verification and validation of EnergyPlus phase change material model for opaque wall assemblies. *Build. Environ.* **2012**, *54*, 186–196. [CrossRef]
35. Designbuilder Natural Ventilation Modelling. Available online: https://designbuilder.co.uk/helpv2/Content/_Natural_ventilation_modelling.htm (accessed on 5 June 2020).
36. Design Builder Mechanical Ventilation. Available online: https://designbuilder.co.uk/helpv4.6/Content/_Air_distribution1.htm (accessed on 5 February 2021).
37. Pajek, L.; Kuni, R.; Ko, M. Improving thermal response of lightweight timber building envelopes during cooling season in three European locations. *J. Clean. Prod.* **2017**, *156*. [CrossRef]
38. Nghana, B.; Tariku, F. Phase change material's (*PCM*) impacts on the energy performance and thermal comfort of buildings in a mild climate. *Build. Environ.* **2016**, *99*, 221–238. [CrossRef]
39. Liu, J.; Liu, Y.; Yang, L.; Liu, T.; Zhang, C.; Dong, H. Climatic and seasonal suitability of phase change materials coupled with night ventilation for of fi ce buildings in Western China. *Renew. Energy* **2020**, *147*, 356–373. [CrossRef]